Preprint
UCRL-JC-136533

X-Ray Absorption Characterization of Diesel Exhaust Particulates

A.J. Nelson, J.L Ferreira, J.G. Reynolds, J.W. Roos

This article was submitted to
Materials Research Society Meeting, Boston, MA, November 29 – December 3, 1999

November 18, 1999

U.S. Department of Energy

Lawrence
Livermore
National
Laboratory

X-RAY ABSORPTION CHARACTERIZATION OF DIESEL EXHAUST PARTICULATES

A. J. NELSON*, J. L. FERREIRA*, J. G. REYNOLDS* and J. W. ROOS**
*Lawrence Livermore National Laboratory, Livermore, CA 94550
**Ethyl Corporation, Richmond, VA 23217

ABSTRACT

We have characterized particulates from a 1993 11.1 Detroit Diesel Series 60 engine with electronic unit injectors operated using fuels with and without methylcyclopentadienyl manganese tricarbonyl (MMT) and overbased calcium sulfonate added. X-ray photoabsorption (XAS) spectroscopy was used to characterize the diesel particulates. Results reveal a mixture of primarily Mn-phosphate with some Mn-oxide, and Ca-sulfate on the surface of the filtered particulates from the diesel engine.

INTRODUCTION

Methylcyclopentadienyl manganese tricarbonyl (MMT) is an effective means of increasing octane quality of gasoline. [1] Comprehensive automotive testing also shows that vehicles using MMT (0.03125 gram manganese per gallon) in gasoline had 6% lower CO emissions and 20% lower NO_x emissions than automobiles operating on base gasoline. [2] In another application, it is proposed that MMT with overbased calcium alkylbenzene sulfonate (OCABS) be employed as a fuel additive package to reduce diesel smoke and particulate emissions. [3] OCABS are also used to impart detergency in engine oils and fuel combustion catalysts. [4,5]

Identification of the manganese and calcium species formed by the decomposition of MMT and OCABS in diesel engines is of practical importance and of environmental interest. These species end up either on surfaces in the exhaust system of an automobile or are emitted into the atmosphere.

This paper reports on an investigation to determine the surface composition of particulates emitted from vehicles operating on fuel containing various concentrations of MMT and calcium sulfonate using X-ray absorption spectroscopy (XAS).

EXPERIMENTAL

Particulate samples from diesel engine test runs using fuels with and without methylcyclopentadienyl manganese tricarbonyl (MMT) and overbased calcium alkylbenzene sulfonate added were characterized. The fuels used were Colonial diesel (389 ppm S) and Howell diesel (460 ppm S). The particulate samples were collected on filter paper. The test runs are summarized in Table I. It should be noted that engine operation time for Run 1716 had a duration five times that of the other test runs resulting in 5X exposure of the filter.

Model compounds were analyzed by XAS and XPS to provide a basis for quantitative analysis of the unknown particulates. The model compounds CaO, $CaCO_3$, $CaSO_4$, $Ca_2P_2O_7$, $Ca(H_2PO_4)_2$, $Ca(NO_3)_2$, $CaCl_2$, MnO, Mn_2O_3, Mn_3O_4, MnO_2, $Mn(OCH_3)_2$, $MnPO_4$, $Mn_5(PO_4)_2[PO_3(OH)]_2 \cdot 4H_2O$ (Mn-Phos) (Alfa Aesar), $Mn(CH_3\ COCH{=}COCH_3)_3$ ($Mn(acac)_3$), MnS (Aldrich) and $MnSO_4 \cdot H_2O$ (Mallinckrodt) were used as received. The powder samples were pressed into indium foil and attached to the sample holder, which was then introduced into the ultra-high vacuum (UHV) chamber for analysis. Similarly, small pieces of the particulate on filter samples were cut and mounted with indium foil on the sample holder prior to their introduction into the analysis chamber.

Table I. Summary of Parameters for Diesel Particulate Test Run Samples

Run Number	Mn (mg Mn/liter)	Ca (mg Ca/liter)	Fuel	Engine Operation Time (min.)
1716	3	18	Colonial	100
1599	50	0	Howell	20
1632	0	50	Howell	20
1605	8	0	Howell	20
1616	0	8	Howell	20
1658	6	36	Howell	20
1591	18	0	Howell	20
1626	0	18	Howell	20

Manganese 2p and calcium 2p core-level XAS were performed on these particulates and the series of Mn and Ca compound standards. This technique probes empty or unfilled 3d electronic states of manganese and provides information on the local chemical environment. For 2p X-ray absorption, the dipole allowed transitions are 2p → 3d and 2p → 4s, with transitions to the 3d states dominating. The observed behavior has been interpreted as the combination of crystal field effects with splittings due to multipole 2p–3d and 3d–3d interactions. Crystal field effects, measured by the cubic crystal field parameter, are equal for both the initial and final states. Also, the 2p core hole spin-orbit coupling splits the absorption spectrum into a $2p_{3/2}$ (L_3) and a $2p_{1/2}$ (L_2) part. In addition, it has been observed that the branching ratio of the L_3 edge intensity to the total line strength depends on the oxidation state of the Mn and Ca. Specifically for Mn, this branching ratio decreases in the order Mn(II) → Mn(III) → Mn(IV). [6,7] This analysis was performed at the 8-2 beam line at the Stanford Synchrotron Radiation Laboratory (SSRL) by scanning the photon energy of the incoming monochromatic synchrotron radiation through the Mn 2p and Ca 2p core-level edge (L-edge) while monitoring the total electron yield. The spectra were calibrated arbitrarily with 640 eV for the absorption maximum in the Mn model compounds and ~347 eV for the Ca model compounds. [8]

RESULTS

XAS – Model Compounds

Figure 1 presents the Mn 2p core level XAS of the Mn model compounds. Analysis of these series of model compounds provides standard Mn L-edge spectra of several formal valences, specifically, Mn(II) in $MnSO_4$, MnO and Mn-Phos, Mn(III) in $MnPO_4$, and a mixture of Mn(II) and Mn(III) in Mn_3O_4. All spectra show two absorption regions, the Mn $2p_{3/2}$ (L_3) at ~640 eV and Mn $2p_{1/2}$ (L_2) at ~650 eV. Characteristic features of the absorption regions depends

upon the ligand environments and the oxidation states. For example, Mn_3O_4 shows a sharp and broad L_3 region and a very broad L_2 region reflecting the oxide environment and the mixture of Mn(II) and Mn(III) oxidation states, while Mn-Phos and $MnSO_4$ show a relatively sharp L_3 region reflecting the single oxidation state Mn(II). Also note the differences in the energy

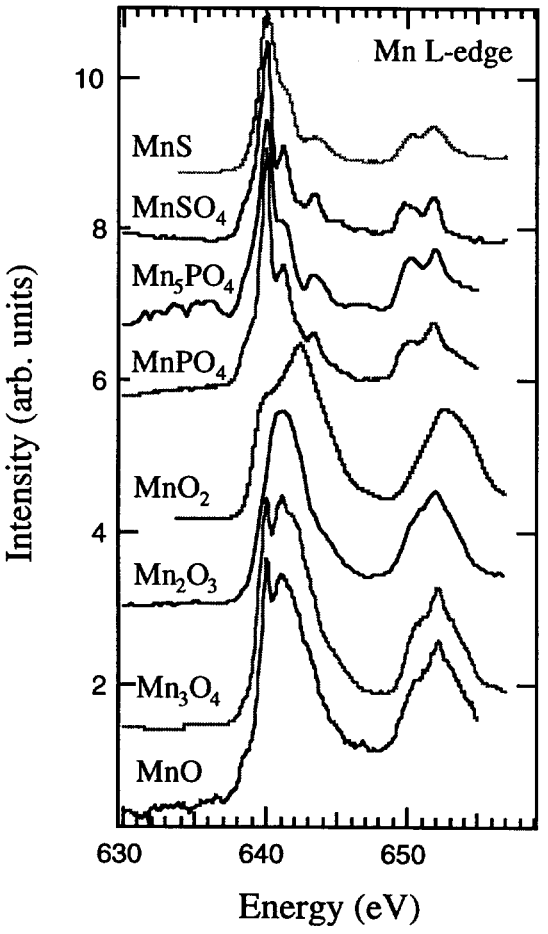

Figure 1. Mn L-edge photoabsorption spectra of model compounds.

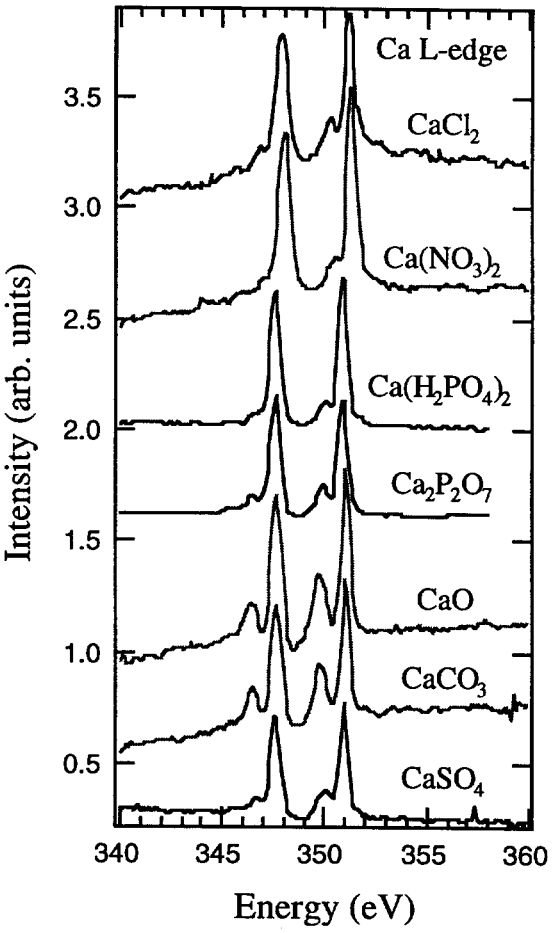

Figure 2. Ca L-edge photoabsorption spectra of model compounds.

separation between the L_3 and L_2 peaks and their relative intensities as well as the shoulder on the low energy side of the L_3 peak for the phosphate and sulfate. Table II summarizes the pertinent Mn L-edge spectral characteristics.

Table II. Summary of the Mn L-edge Spectral Features for Mn Model Compounds.

Compound	Formal Mn Valency	$\Delta E(L_3 - L_2)$ (eV)	L_3 Linewidth FWHM (eV)	Branching Ratio $I(L_3)/I(L_3 + L_2)$
MnO	II	12.0	4.2	0.60
Mn_3O_4	II, III	12.0	4.2	0.62
Mn_2O_3	III	11.0	3.8	0.62
MnO_2	IV	10.2	5.3	0.61
$MnPO_4$	III	11.8	1.0	0.78
Hureaulite[a]	II	11.8	1.3	0.78
$MnSO_4$	II	11.8	1.1	0.82
MnS	II	11.8	1.6	0.82

a) $Mn_5(PO_4)_2[PO_3(OH)]_2 \cdot 4H_2O$.

Figure 2 presents the Ca 2p core level XAS of the Ca model compounds. All spectra show two areas of absorption, Ca $2p_{3/2}$ (L_3) at ~348 eV and Ca $2p_{1/2}$ (L_2) at ~351 eV. Also, smaller associated absorptions are seen as either shoulders or resolved satellite peaks for both L_3 and L_2 in all spectra. Quantitative determination of the model compound Ca species relies on energy separations of the small satellite peak and the associated main peak of the Ca L-edge spectra as are summarized in Table III. Since Ca only occurs as Ca(II), subtle differences in the peak shapes, $\Delta E(L_{3a} - L_{3b})$, linewidths and the branching ratio will be utilized to determine Ca speciation in the diesel particulates.

Table III. Summary of the Ca L-edge Spectral Features for Ca Model Compounds.

Compound	$\Delta E(L_3 - L_2)$ (eV)	$\Delta E(L_{3a} - L_{3b})$ (eV)	L_3 Linewidth FWHM (eV)	Branching Ratio $I(L_3)/I(L_3 + L_2)$
$CaSO_4$	3.4	0.8	0.6	0.46
CaO	3.4	1.2	0.7	0.45
$CaCO_3$	3.4	1.1	0.7	0.46
$Ca_2P_2O_7$	3.2	1.1	0.7	0.50
$Ca(H_2PO_4)_2$	3.2	0.8	0.7	0.48
$Ca(NO_3)_2$	3.2	0.8	0.8	0.43
$CaCl_2$	3.3	1.0	0.8	0.46

XAS Analysis – diesel particulates

The Mn XAS spectra for the diesel particulate samples are presented in Figure 3. Table IV summarizes the spectral characteristics. From visual comparison, these spectra best match the Mn L-edge spectrum for Mn_2O_3. The L_3 linewidth suggests a mixture of species, most likely containing oxide. The L_3–L_2 energy separation suggests pure oxides or a mixture of oxides and other species such as phosphate and sulfate. The branching ratios suggest a mixture of phosphate and/or sulfate with oxides.

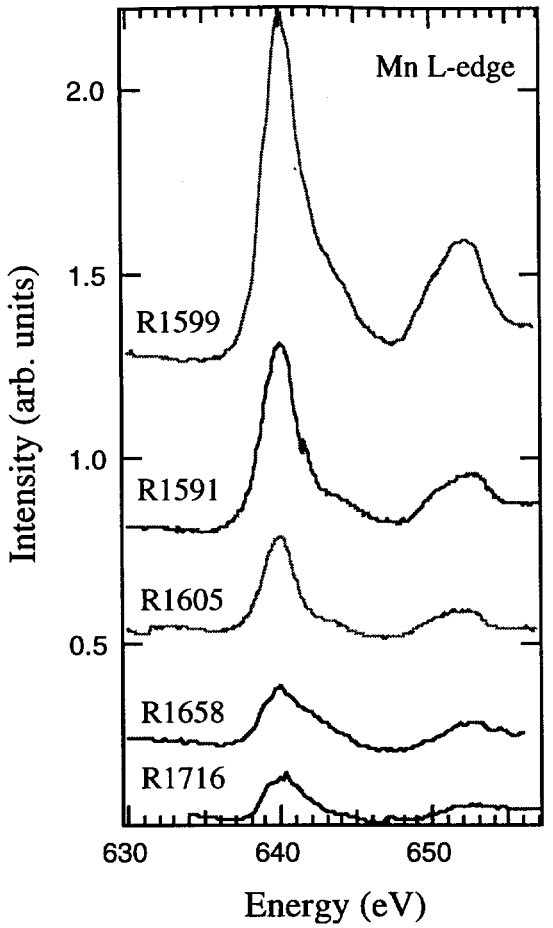

Figure 3. Mn L-edge photoabsorption spectra of diesel particulates.

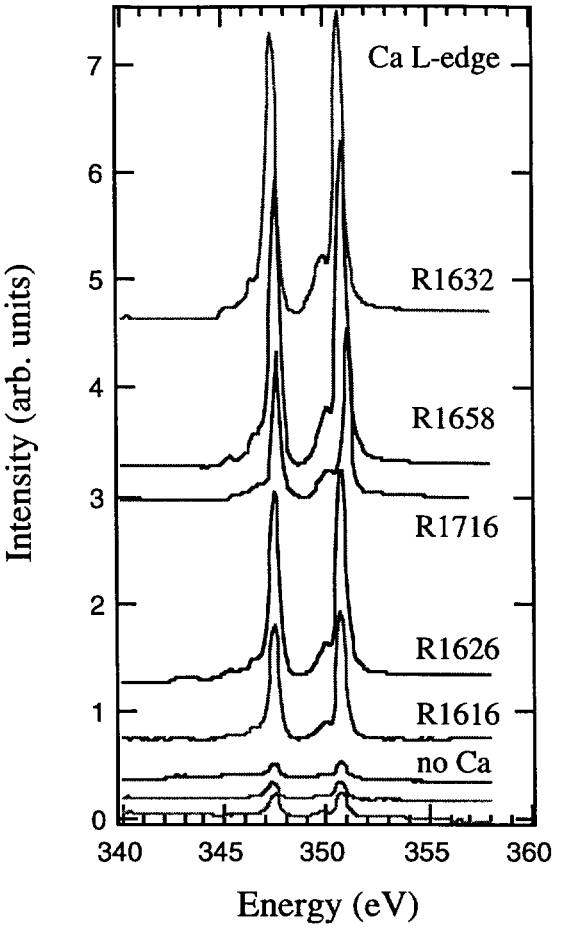

Figure 4. Ca L-edge photoabsorption spectra of diesel particulates.

Table IV. Summary of the Mn L-edge Spectral Features for Diesel Particulates

Sample	$\Delta E(L_3 - L_2)$ (eV)	L_3 Linewidth FWHM (eV)	Branching Ratio $I(L_3)/I(L_3 + L_2)$
Run 1716	12.0	3.2	0.73
Run 1599†	12.0	3.2	0.77
Run 1632‡	–	–	–
Run 1605†	12.0	2.7	0.79
Run 1616‡	–	–	–
Run 1658	12.0	3.2	0.67
Run 1591†	12.0	2.8	0.79
Run 1626‡	–	–	–

†no Ca added to fuel, ‡no Mn added to fuel

The Ca XAS spectra for the diesel particulate samples are presented in Figure 4. Table V summarizes the spectral characteristics. Visual comparison of the Ca L_3 spectral features for the diesel particulates with the Ca L_3 spectral features for the Ca model compounds would seem to indicate that the Ca speciation has several possibilities and that the species may be different for some of the samples. The L_3 linewidth suggests in all cases $CaSO_4$. The L_3–L_2 energy separation suggests phosphate and nitrate (chloride is most likely not occurring because of the lack of a chloride source). The L_{3a}–L_{3b} satellite separation suggests sulfate, phosphate, and nitrate. The branching ratio suggests phosphate and sulfate.

Table V. Summary of the Ca L-edge Spectral Features for the Diesel Particulates

Sample	$\Delta E(L_3 - L_2)$ (eV)	$\Delta E(L_{3a} - L_{3b})$ (eV)	L_3 Linewidth FWHM (eV)	Branching Ratio $I(L_3)/I(L_3 + L_2)$
Run 1716	3.5	1.0	0.5	0.47
Run 1599†	–	–	–	–
Run 1632‡	3.3	1.0	0.6	0.49
Run 1605†	–	–	–	–
Run 1616‡	3.2	0.9	0.6	0.47
Run 1658	3.2	1.0	0.6	0.48
Run 1591†	–	–	–	–
Run 1626‡	3.3	0.9	0.6	0.47

†no Ca added to fuel, ‡no Mn added to fuel

CONCLUSIONS

We have applied XAS to identify Mn and Ca species in exhaust particulates from a diesel engine operated using fuel with MMT and overbased calcium alkylbenzene sulfonate. These compounds are reported to improve combustion characteristics leading to reduced diesel smoke and particulate emissions.

We have compared the energy separation of the XAS L_3 and L_2 edges, the L_3 linewidth, and the branching ratio of these diesel samples with the spectral characteristics of the Mn and Ca model compounds to determine the surface composition of the samples. Results for the diesel particulate samples indicate that the Mn is present as a mixture of phosphate and/or sulfate with oxides and that the Ca is primarily present as $CaSO_4$, consistent with the higher operating temperatures. A high sulfur content fuel and diesel operating conditions would probably yield primarily sulfates. However, Ethyl simulations indicate that $MnSO_4$ is not stable at higher temperatures.

Acknowledgments

The XAS work was performed at the Stanford Synchrotron Radiation Laboratory, which is supported by the U.S. Department of Energy, Office of Basic Energy Sciences, under Contract No. DE-AC03-76SF00515.

REFERENCES

1. J. E. Faggan, J. D. Bailie, E. A. Desmond and D. L. Lenane, SAE Paper 750925 (1975), Warrenville, PA: Society for Automobile Engineering.
2. D. P. Hollrah and A. M. Burns, Oil & Gas Journal, March 11, 1991, pp. 86–90.
3. G.R. Wallace, Hydrocarbonaceous Fuel Composition and Additives Thereof, US Pat 5944858.
4. G.G. Pritzker, Natl. Petroleum News **37**, 793 (1945).
5. J.F. Marsh, Colloidal lubricant additives, Chem. Ind. (London, 1987) p. 470.
6. S.P. Cramer, F.M.F. deGroot, Y. Ma, C.T. Chen, F. Sette, C.A. Kipke, D.M. Eichhorn, M.K. Chan, W.H. Armstrong, E. Libby, G. Christou, S. Brooker, V. McKee, O.C. Mullins and J.C. Fuggle, J. Am. Chem. Soc. **113**, 7937 (1991).
7. M.M. Grush, J. Chen, T.L. Stremmler, S.J. George, C.Y. Ralston, R.T. Stibrany, A. Gelasco, G. Christou, S.M. Gorun, J.E. Penner-Hahn and S.P. Cramer, J. Am. Chem. Soc. **118**, 65 (1996).
8. Zhanfeng Yin, M. Kasrai, G.M. Bancroft, K. Fyfe, M.L. Colaianni and K.H. Tan, Wear **202**, 192 (1997).

This work was performed under the auspices of the U.S. Department of Energy by the University of California, Lawrence Livermore National Laboratory under Contract No. W-7405-Eng-48.